TU/e EINDHOVEN UNIVERSITY OF TECHNOLOGY

Si/XeF2 etching: Temperature dependence

Citation for published version (APA):
Vugts, M. J. M., Verschueren, G. L. J., Eurlings, M. F. A., Hermans, L. J. F., & Beijerinck, H. C. W. (1996). Si/XeF2 etching: Temperature dependence. *Journal of Vacuum Science and Technology A*, *14*(5), 2766-2774. https://doi.org/10.1116/1.580198

DOI:
10.1116/1.580198

Document status and date:
Published: 01/01/1996

Document Version:
Publisher's PDF, also known as Version of Record (includes final page, issue and volume numbers)

Please check the document version of this publication:

• A submitted manuscript is the version of the article upon submission and before peer-review. There can be important differences between the submitted version and the official published version of record. People interested in the research are advised to contact the author for the final version of the publication, or visit the DOI to the publisher's website.
• The final author version and the galley proof are versions of the publication after peer review.
• The final published version features the final layout of the paper including the volume, issue and page numbers.

Link to publication

General rights
Copyright and moral rights for the publications made accessible in the public portal are retained by the authors and/or other copyright owners and it is a condition of accessing publications that users recognise and abide by the legal requirements associated with these rights.

• Users may download and print one copy of any publication from the public portal for the purpose of private study or research.
• You may not further distribute the material or use it for any profit-making activity or commercial gain
• You may freely distribute the URL identifying the publication in the public portal.

If the publication is distributed under the terms of Article 25fa of the Dutch Copyright Act, indicated by the "Taverne" license above, please follow below link for the End User Agreement:

www.tue.nl/taverne

Take down policy
If you believe that this document breaches copyright please contact us at:

openaccess@tue.nl

providing details and we will investigate your claim.

Download date: 16. Nov. 2023

Si/XeF_2 etching: Temperature dependence

M. J. M. Vugts, G. L. J. Verschueren, M. F. A. Eurlings, L. J. F. Hermans, and H. C. W. Beijerinck[a)]
Physics Department, Eindhoven University of Technology, P.O. Box 513, 5600 MB Eindhoven, The Netherlands

(Received 7 July 1995; accepted 13 May 1996)

The temperature dependence of the $Si(100)/XeF_2$ etch reaction is studied quantitatively in a molecular beam setup. At a sample temperature of 150 K the reaction probability reaches unity initially, after which the XeF_2 condenses on the surface and blocks the etching process. For increasing temperatures the XeF_2 reaction probability initially decreases from 100% at 150 K down to 20% around 400 K, but for temperatures above 600 K it increases again up to 45% at 900 K. In a simple reaction scheme the high etch rate at low temperatures is explained by a XeF_2-precursor, with an activation energy for desorption of 32 ± 4 meV. Furthermore the increased etch rate at high temperatures is explained by the desorption of SiF_2 with an activation energy of 260 ± 30 meV. The steady-state fluorine content of the SiF_x reaction layer, measured using thermal desorption spectroscopy, reaches a maximum of 5.5 monolayers at 300 K. For increasing temperatures it decreases to a submonolayer coverage above 700 K. The temperature dependence of the formation of the reaction layer is described well by including the XeF_2-precursor in a previously developed adsorption model. © *1996 American Vacuum Society.*

I. INTRODUCTION

Plasma etching is one of the most important steps in the fabrication process of integrated circuits, and fluorine is the main etchant in many of these plasmas. Therefore many surface science studies have been devoted to the interaction of fluorine species with silicon, in order to unravel the fundamental physics and chemistry of the etching process.[1]

The XeF_2 molecule has been frequently used in these studies as a convenient source of fluorine atoms. It is a solid with a vapor pressure of 4.5 Torr at 300 K. At the silicon surface the XeF_2 dissociates, which results in the formation of a silicon fluoride reaction layer.[2] X-ray photoelectron spectroscopy (XPS) experiments showed that this layer consists of SiF-, SiF_2- and SiF_3-species.[3,4] Initially there was some disagreement on the thickness of this layer. From high resolution XPS-experiments it was estimated to be 4 monolayers of fluorine atoms,[5] in which the unit monolayer (ML) is defined as the surface density of the sample studied [Si(100): 1 $ML=6.86\times10^{18}$ m^{-2}]. Other groups, however, reported layers as thick as 13 ML (Refs. 1 and 6) and even a value of 38 ML was reported by our group using thermal desorption spectroscopy (TDS).[7] But these large values are probably the result of surface roughening caused by the etching process, as was shown to be the case for our experiments in a subsequent study.[8] In that study it was also shown that the reaction layer formation is a function of the XeF_2-dose only, independent of flux, and can be described by distinguishing two regimes. For the first 100 ML of XeF_2-exposure a monolayer of SiF_x-species is formed, which changes into a multilayer of Si_xF_y-chains upon further exposure. Steady state is reached around 25 000 ML, when the reaction layer consists on the average of SiF-SiF_2-SiF_3- and SiF_2-SiF_3-chains.[5,8] In this steady state situation 20% of the incident XeF_2 is used in the etch-reaction at room temperature. The main etch product is SiF_4 with minor contributions from more fluorinated species like Si_2F_6 and Si_3F_8.[1,9,10]

So far most temperature dependence studies of the Si/XeF_2-reaction have concentrated on the product distribution. It was shown by Dagata *et al.*[11] that above 600 K SiF_2 becomes a significant etch product. Experiments in our setup[7] showed that this is accompanied by an increase in the XeF_2 reaction probability to a value of 50% at 900 K and a slight decrease in the SiF_4-production. In the temperature range from 300 to 1000 K, Winters and Coburn[1] observed a minimum in the reaction probability around 400 K. A similar effect was observed by Ibbotson *et al.*[12] but it is hard to compare this experiment with the beam work because it was done in a completely different (non-UHV) regime, using a XeF_2 pressure of 10^{-1} Torr. No data have been reported for sample temperatures below 260 K.

Few experiments were done to study the temperature dependence of the steady state reaction layer. Bermudez[13] observed, using infrared reflection absorption spectroscopy, that between 300 K and 550 K the reaction layer consists of SiF-, SiF_2- and SiF_3-species, while at higher temperatures the SiF-coverage increases as other species decompose. Using Auger electron spectroscopy (AES) and XPS, Chuang[14] found that XeF_2 chemisorption on Si is still dissociative at -150 °C.

We conclude that the knowledge on the temperature dependence of the Si/XeF_2-reaction is still very limited. More information on this subject will help us to understand the essentials of the reaction mechanisms, also at room temperature. Furthermore, there has recently been an increasing interest in low temperature plasma etching as a high anisotropy, low damage technique.[15–20] This motivated the detailed study on the temperature dependence of both the product distribution and the reaction layer dynamics which is described in this article.

[a)]Electronic mail: H.C.W.Beijerinck@phys.tue.nl

In the next section a brief description of the experimental setup will be given. In sections III, IV and V the experimental data on the temperature dependence of the steady state reaction layer, the formation of this layer, and the etch rate will be presented. Subsequently these data will be discussed in terms of reaction mechanisms in section VI and finally we will summarize our conclusions in section VII.

II. EXPERIMENTAL SETUP

The experiments were done in a multiple beam setup that was described in detail in a previous article.[7] Therefore we will just give a short description of the elements that were used in this study.

The samples studied were all n-type (phosphorus, 2–3 Ω cm) Si(100)-surfaces. After a sample was cleaned with HF to remove native oxide, it was mounted in a UHV chamber, having a background pressure below 10^{-8} Torr. The nickel sample holder can be temperature controlled from 100 K up to 1000 K. A temperature ramp of 2 K s^{-1} can be applied fast enough for thermal desorption experiments. Several samples were used and each sample was used for several experiments. Before each experiment the sample was heated to 900 K to remove all remaining fluorine. In order to verify that the samples were not contaminated by nickel from the sample holder, some samples were transferred to a different setup after the experiments and subjected to Auger- and XPS-analysis. No traces of nickel or any other metal could be found, indicating that the influence of contaminants is negligible.

The XeF_2 was supplied by means of an effusive gas source at an angle of 52° with the surface normal. The XeF_2-flux was calculated from the XeF_2 vapor pressure and the dimensions of the gas source. It can be varied from 0.06 ML s^{-1} up to 3.6 ML s^{-1} on the 3 mm diameter detection area of the sample.

Species desorbing from the detection area of the sample are detected by a quadrupole mass spectrometer, which is positioned in a separate UHV chamber with a background pressure below 10^{-9} Torr. The detector chamber is separated from the sample chamber by means of two flow resistances and a differential pumping stage. This ensures that a large fraction ($\approx$85%) of the detection signal is due to species desorbing directly from the sample. The mass spectrometer signals that were used in these experiments were SiF_3^+ for SiF_4, SiF^+ for SiF_2, and XeF^+ or XeF_2^+ for XeF_2-desorption. These signals were all corrected for background influences and the temperature dependence of the detection probability as described in a previous article.[7] That article also described the calibration of the signals using an inert nickel mounting plate and a F-atom mass balance for the steady state signals. The detection efficiency was typically 10^{-4} ML $count^{-1}$.

Thermal desorption spectroscopy was used to analyze the SiF_x reaction layer. This was done by heating the sample after XeF_2 exposure up to 900 K with a ramp of 2 K s^{-1} while monitoring the SiF_4-desorption. By integrating these thermal desorption spectra the original fluorine content L of the layer was determined. This technique was also used to monitor the roughening of the sample during the etching process. In order to correct the experiments for the surface roughness, the fluorine content L was scaled to the fluorine content L_{cal} of a calibration experiment which was repeated frequently during the measurements[8]:

$$\mathscr{L} = \frac{L}{L_{cal}}. \tag{1}$$

This calibration experiment consisted of an exposure of the clean sample at 300 K to a XeF_2-flux of 1.0 ML s^{-1} for 3000 s followed by a thermal desorption experiment. Since we assume that L_{cal} is proportional to the effective surface area, the scaled fluorine content $\mathscr{L}$ will be independent of surface roughness. During the experiments described in this article, the surface roughness (L_{cal}) showed an overall increase, as the sample aged. However, in contrast to the room temperature experiments,[8] the increase was not monotonic but showed some fluctuations. Possibly this is related to the large variation in etch rate over the temperature range studied (section V).

III. STEADY-STATE REACTION LAYER

For Si/XeF_2 etching at room temperature it was established that a XeF_2-dose of 25 000 ML is necessary to reach a steady-state reaction layer.[5,8] With the XeF_2-fluxes that can be reached in our experiment this means a detailed study of the temperature dependence of the reaction layer would take several days. Since the sample severely roughens from one day to the next,[8] this would complicate a comparison between the experiments. As a compromise we chose to limit the dose to 2400 ML at each temperature as an indication of the steady-state behavior. The experimental procedure was the following. First the sample was cleaned by heating to 900 K, and then it was cooled to the desired temperature. Subsequently the sample was exposed for 2400 s to a XeF_2-flux of 1 ML s^{-1}. After this a thermal desorption spectrum was taken and the sample was cooled again to start a new experiment. This was done for sample temperatures ranging from 150 K to 900 K.

The evolution of the TDS-spectra below room temperature is shown in Fig. 1. The 300 K spectrum shows the familiar two-peak structure which was also observed in previous experiments[8]: an α-peak around 500 K and a β-peak around 700 K. From the behavior of these peaks as a function of sample history it was concluded that the β-peak results from tightly bound species and the α-peak from loosely bound species at corrugated sites. This two-peak structure does not change significantly with decreasing temperature but a new feature appears at the low temperature side of the spectrum. This ''γ-peak'' becomes dominant around 175 K and even exceeds the maximum count rate of the detector for the etching data at 150 K (not shown). When we compare this with the XeF_2 desorption signal monitored simultaneously after 400 ML of exposure at 175 K, it is clear that the γ-feature in the SiF_4-spectra is related to a large XeF_2-desorption signal (Fig. 2). Using different temperature ramps

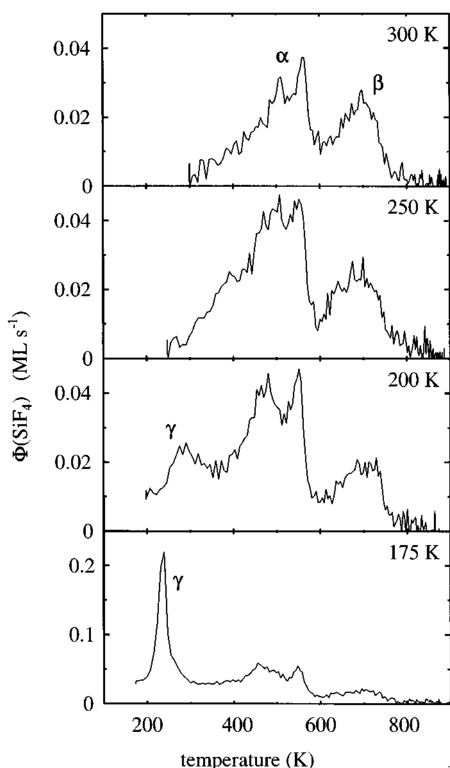

FIG. 1. Thermal desorption spectra after a XeF$_2$-dose of 2400 ML for sample temperatures of 300 K, 250 K, 200 K, and 175 K. Note the difference in vertical scales.

and Redhead's peak maximum method,[21] we determined the desorption energy E_γ of the γ-peak:

$$E_\gamma = 580 \pm 10 \text{ meV}. \tag{2}$$

This corresponds to the vaporization energy of XeF$_2$ ($E_{XeF_2} = 573 \pm 8$ meV).[22] Therefore we conclude that the γ-feature is caused by the evaporation of a XeF$_2$ condensation layer on the silicon surface. This yields a large SiF$_4$ desorption signal by direct reaction of the evaporating XeF$_2$. Similar halogen condensation effects have been observed by Jackman *et al.* for bromine and iodine etching of silicon at 100 K.[23]

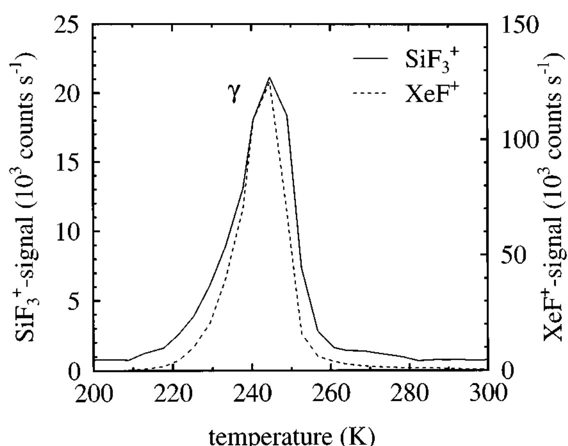

FIG. 2. The γ-peak in the TDS-spectra of both SiF$_4$ (SiF$_3^+$-signal) and XeF$_2$ (XeF$^+$-signal) after a XeF$_2$-dose of 400 ML at 175 K.

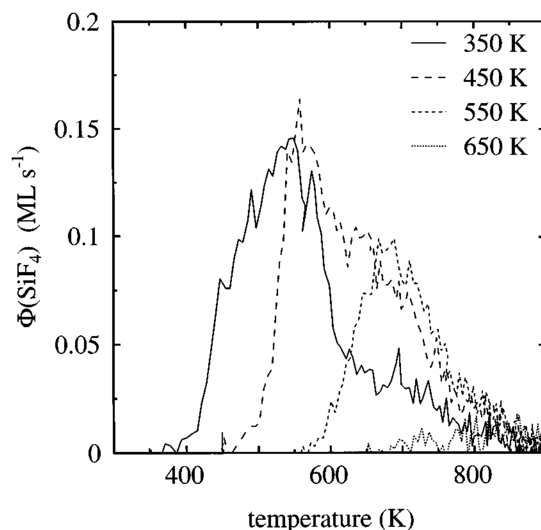

FIG. 3. Thermal desorption spectra after a XeF$_2$-dose of 2400 ML for sample temperatures of 350 K, 450 K, 550 K, and 650 K.

Figure 3 shows the behavior of the TDS-spectra above room temperature. The α-peak is higher than in Fig. 1, presumably because this series was done on a rougher surface.[8] Apart from the fact that there is, of course, no desorption below the etch temperature, we observe an increase in the desorption at higher temperatures for the 450 K and 550 K spectra. This indicates a shift to more tightly bound species. The 650 K spectrum shows a strong decrease in the desorption signal.

The overall behavior of the scaled fluorine content $\mathcal{L}$ after 2400 ML of XeF$_2$-exposure is shown in Fig. 4. The fluorine content seems to saturate below room temperature,

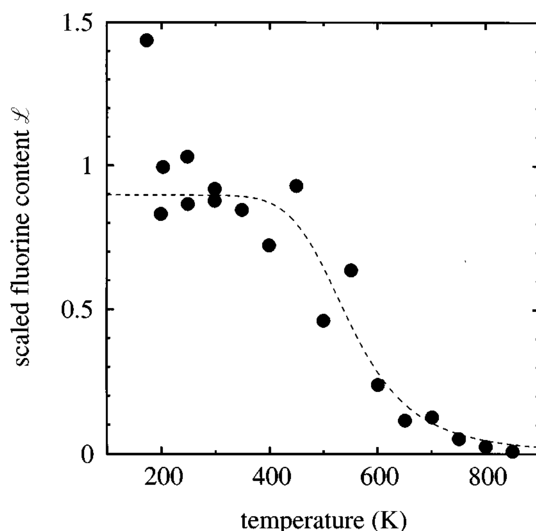

FIG. 4. The scaled fluorine content after a XeF$_2$-dose of 2400 ML at various temperatures, as determined from integrated TDS-spectra. The dashed curve indicates the observed trend.

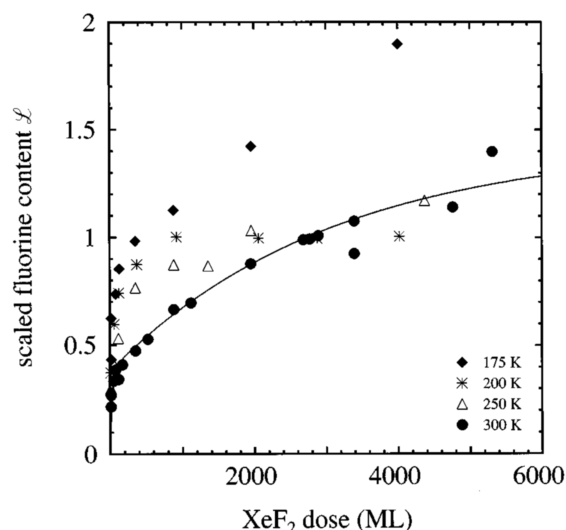

FIG. 5. Scaled fluorine content $\mathscr{L}$ of the reaction layer as a function of XeF_2-dose for sample temperatures of 300 K and below. The solid curve represents the fit with the chain model for the 300 K data, which was determined in a previous study (Ref. 8).

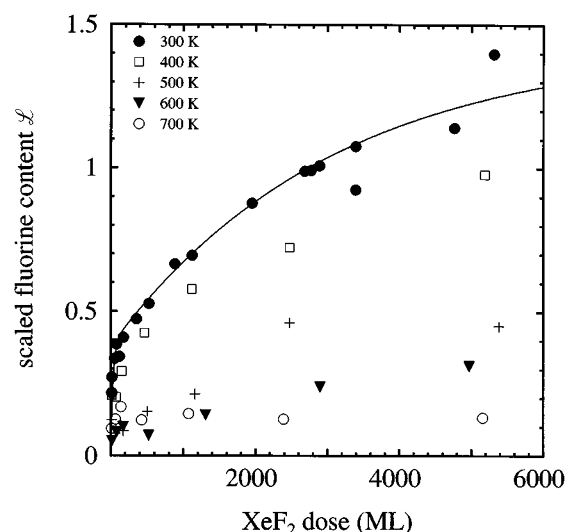

FIG. 6. Scaled fluorine content $\mathscr{L}$ of the reaction layer as a function of XeF_2-dose for sample temperatures of 300 K and above. Again the solid curve represents the fit with the chain model for the 300 K data (Ref. 8).

down to around 175 K. As seen above, the large content at this temperature is due to XeF_2-condensation on the surface, as observed by a strong increase in the γ-peak. Above room temperature $\mathscr{L}$ shows a sharp decrease around 500 K. For temperatures of 800 K and higher the desorption is hardly significant.

IV. FORMATION OF THE REACTION LAYER

As in our previous experiments on room temperature etching,[8] we studied the formation of the reaction layer for different sample temperatures by measuring the fluorine content as a function of XeF_2-dose. A clean sample was heated or cooled to the desired temperature, and then it was exposed to a XeF_2-flux of 1.0 ML s^{-1} for a period ranging from 100 to 6000 s. Subsequently a TDS-spectrum was taken, which was integrated to determine the fluorine content L of the layer. During the longer measurements (>2000 s) the detection area was occasionally switched to the nickel plate, for calibration of the detector signals.[7] Each temperature series took one day of experimenting and was sandwiched between two calibration experiments, as described in the previous section, to monitor the surface roughness and determine the scaled fluorine content $\mathscr{L}$ [Eq. (1)].

In Fig. 5 the results for low temperatures are shown. The scaled fluorine content $\mathscr{L}$ is plotted as a function of XeF_2-dose (dose=flux×time) for temperatures of 300 K, 250 K, 200 K, and 175 K. The solid curve is the fit for the 300 K data with the chain model, which was introduced in a previous study.[8] This model describes the reaction layer formation at room temperature as a two-stage process, a fast formation of SiF_x-adsorbates followed by a slow transition to a structure of Si_xF_y-chains. It is based on previous TDS-experiments by our group[8] and on the ''tree-structure'' of the reaction layer as proposed by Lo *et al.*[5] More details are presented in section VI B.

We observe in Fig. 5 that for 250 K and 200 K the initial growth of the reaction layer is much faster than at room temperature. Furthermore, especially for the 200 K data, the reaction layer seems to saturate at a much lower XeF_2-dose and fluorine content. The 175 K data show a different behavior. The fast initial growth rate is followed by a linear increase in the fluorine content. As was shown in the previous section, this can be explained by XeF_2-condensation on the surface.

The high temperature data are displayed in Fig. 6. For comparison the 300 K data of Fig. 5 are repeated. The fluorine content is seen to decrease with increasing temperature, but the qualitative behavior of the 400 K, 500 K and 600 K data is very similar to what was observed at room temperature. At 700 K the fluorine content seems to saturate almost immediately. Above 700 K the desorption signal was too weak to allow a study of the dose dependence.

V. STEADY-STATE REACTION

During the XeF_2 exposure in the experiments of the previous section, we monitored the reaction products using the mass spectrometer signals. From the steady state levels of these signals we can determine the reaction coefficient and the product distribution. We define the reaction coefficient ϵ as the flux of fluorine used at the sample normalized to the total flux of fluorine arriving at the sample:

$$\epsilon=\frac{\Phi_s(XeF_2)-\Phi(XeF_2)}{\Phi_s(XeF_2)}, \tag{3}$$

with $\Phi_s(XeF_2)$ the flux of XeF_2 arriving at the sample from the gas source and $\Phi(XeF_2)$ the nonused flux of XeF_2 leaving the sample. As was described in a previous paper,[7] the reaction coefficient can be determined quite easily in our

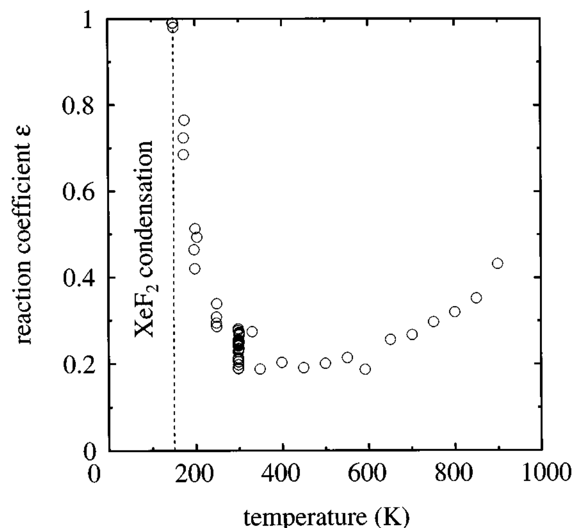

FIG. 7. Temperature dependence of the steady state reaction coefficient ϵ. The XeF$_2$-flux was typically 1 ML s^{-1}. For sample temperatures of 150 K and below the XeF$_2$ condenses on the surface, and the term ''reaction coefficient'' is no longer appropriate.

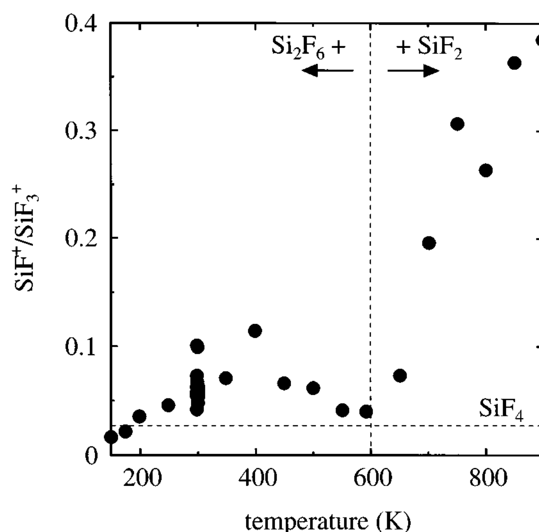

FIG. 8. Steady-state ratio of the SiF_3^+ and SiF^+ mass spectrometer signals as a function of sample temperature. The dashed horizontal corresponds to a ratio of $SiF_3^+/SiF^+=0.027$, which was measured for pure SiF_4-gas in our experiment.

experiment by the use of an inert nickel reference surface. The results for the temperature dependence of the reaction coefficient are shown in Fig. 7. We observe a minimum of $\epsilon=0.20$ around 400 K. For higher temperatures ϵ increases up to $\epsilon=0.45$ at 900 K. For decreasing temperatures the reaction coefficient shows a much stronger increase up to the maximum value of $\epsilon=1$ for temperatures of 150 K and below, where the XeF$_2$ condenses on the surface. At 300 K, where all the calibration experiments were done, a lot of data points are available. The spread in these points gives an indication of the reproducibility of the data and the large influence of sample history and experimental conditions on the measurements.

In our experiment we only have the SiF_3^+ and SiF^+ mass spectrometer signals available to determine the product distribution. The ratio of these two signals during steady state etching is shown in Fig. 8 as a function of sample temperature. For comparison we also measured the SiF^+/SiF_3^+-ratio for pure SiF_4-gas, indicated by the dashed horizontal for $SiF^+/SiF_3^+=0.027$. The signal ratio shows a complex temperature dependence. From a value close to that of pure SiF_4 at 150 K it increases, reaching a maximum at 400 K, followed by a decrease reaching a minimum around 600 K after which it increases sharply. Over the whole range from 200 K up to 900 K the ratio is larger than the ratio for SiF_4. This means that apart from SiF_4 other etch-products are involved. The high ratio above 600 K is explained by SiF_2-production,[12] resulting in an increase of the SiF^+-signal compared to that from pure SiF_4. The high ratio around 400 K is probably explained by the production of more fluorinated species like Si_2F_6 and Si_3F_8, as was observed in temperature dependent F-atom experiments by Winters and Coburn.[1] However, we were not able to confirm this: the $Si_2F_5^+$-signal could not be measured since it overlaps with the XeF^+-signal and $Si_3F_7^+$ was never detected above background. Using the signal ratio for pure Si_2F_6 [$SiF_3^+/SiF^+=2.70$ (Ref. 24)] it can be calculated that the Si$_2$F$_6$-contribution is less than 10% over the whole range.

Now we want to translate the SiF_3^+ and SiF^+ mass spectrometer signals into fluxes of etch-products desorbing from the sample. For this purpose we assume that SiF_4 is the only etch-product below 600 K (neglecting the small Si_2F_6-contribution) and that SiF_2 is only significant above 600 K. Analogous to the reaction coefficient ϵ, we introduce the production coefficient δ as the flux of fluorine atoms produced (i.e., bound to desorbing products), normalized to the total flux of fluorine atoms arriving at the sample. In this case the production coefficient consists of two contributions:

$$\delta=\delta_4+\delta_2, \tag{4}$$

with

$$\delta_4=\frac{2\Phi(SiF_4)}{\Phi_s(XeF_2)}, \quad \delta_2=\frac{\Phi(SiF_2)}{\Phi_s(XeF_2)}, \tag{5}$$

in which $\Phi(SiF_4)$ is the SiF_4-flux and $\Phi(SiF_2)$ is the SiF_2-flux desorbing from the sample. Since we only consider the steady state signals, the flux of fluorine reacting as XeF$_2$ equals the flux of fluorine produced as etch products, and thus

$$\epsilon=\delta. \tag{6}$$

Using this steady-state condition, the SiF_3^+- and SiF^+-signals can be calibrated and δ_4 and δ_2 can be calculated, as was described previously.[7] The temperature dependence of δ_4 and δ_2 is shown in Fig. 9. The SiF_4 production coefficient decreases exponentially from $\delta_4=1.0$ at 150 K down to $\delta_4=0.15$ at 900 K. The SiF_2 production shows a strong increase starting from 600 K up to $\delta_2=0.30$ at 900 K.

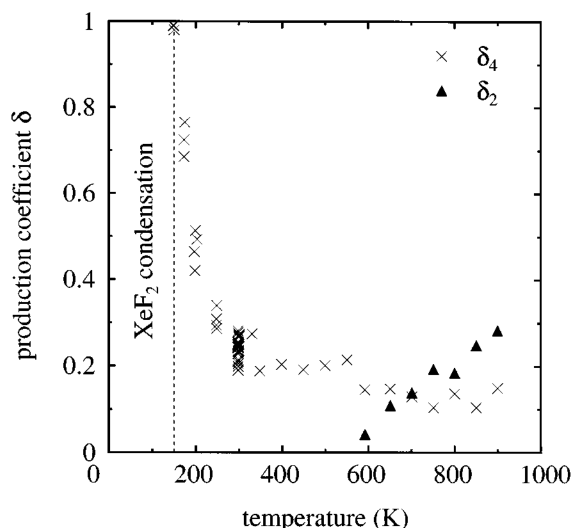

FIG. 9. Temperature dependence of the production coefficients δ_4 for SiF_4-production and δ_2 for SiF_2-production. The XeF_2-flux was typically 1 ML s^{-1}. For sample temperatures of 150 K and below XeF_2-condensation eventually blocks the reaction.

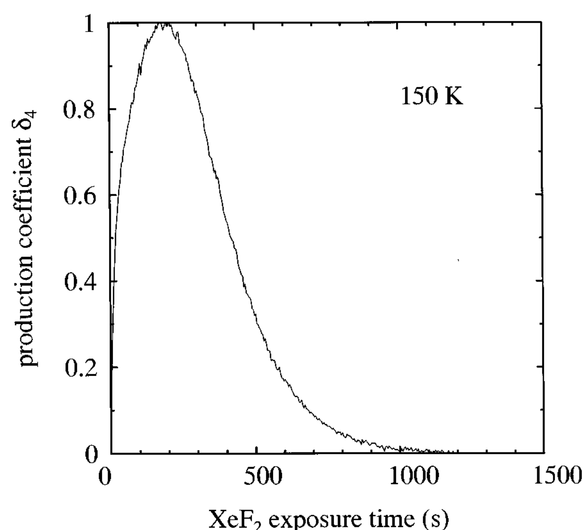

FIG. 10. Time dependence of the production coefficient δ_4 for exposure of a clean sample at 150 K to a XeF_2 flux of 0.9 ML s^{-1}.

As was concluded in section III, a fraction of the incident XeF_2 condenses on the silicon surface for sample temperatures of 200 K and below. This implies that the steady state condition of Eq. (6) is no longer valid at these temperatures and the calculated production coefficients must be considered to be an upper limit. From the intensity of the γ-peak (Fig. 1), we estimate this deviation to be 0.1% at 200 K, 1.1% at 175 K, while at 150 K the XeF_2 condensation rate is so large that it prohibits steady state etching. The time dependence of δ_4 at 150 K is shown in Fig. 10. The production coefficient shows a strong increase for the first 200 s of exposure, reaching a maximum close to $\delta_4 = 1.0$. This means we have a very efficient etching process, in which all of the incident XeF_2 is used to produce etch products. However, after 200 s of exposure the production coefficient starts to decrease and after 1200 s the etching process stops. From the high initial value we deduce that the low sample temperature is not a barrier for the etching process. Therefore we conclude that the release of products is eventually stopped by the small fraction of XeF_2 which condenses on the surface, forming a blocking XeF_2 overlayer. This seems to be in contradiction with the experiments by Chuang,[14] who observed dissociative chemisorption of XeF_2 even at 123 K. We presume that either the XeF_2 dose, which was not reported, was much lower in those experiments or that the Auger- or XPS-analysis itself is causing the condensed XeF_2 to dissociate.

VI. DISCUSSION

The reaction of XeF_2 with silicon has a very complex nature, as is shown by the number of products that are involved,[1] the dose dependence of reaction layer and etch rate,[5,8] the influence of doping,[9,25,26] and the dependence on sample temperature.[12] Therefore a detailed modelling of the reaction is not feasible. Instead we will try to indicate the rate-limiting steps for the steady state etching process[27,28] and describe the reaction layer formation within the framework of the chain model.[8]

A. Reaction mechanism

The Si/XeF_2-etch rate shows a complex temperature dependence. As the temperature is increased from 150 K, it initially decreases, reaches a minimum around 400 K and subsequently increases (Figs. 7 and 9). The minimum around 400 K has also been observed in the experiments at room temperature and above by Ibbotson *et al.*[12] and by Winters and Coburn.[1] Both studies attribute the increased etch rate at temperatures below 400 K to a reaction mechanism involving a XeF_2-precursor. This seems reasonable considering the low temperature effects observed in our experiments. Ibbotson *et al.*[12] suggest that the increase at high temperatures is caused by a change in the reaction mechanism towards direct impact dissociation of the XeF_2. However, we observed that the increase in the etch rate at high temperatures is correlated with the breakdown of the SiF_x reaction layer (Fig. 4) and the production of SiF_2 (Fig. 9). Therefore we suspect that the desorption of SiF_2, and thus the increase in reactive sites at the surface, is the actual cause of the increased etch rate at high temperatures.

The simplest conceivable reaction mechanism[27] that implements these ideas consists of 4 main steps (we neglect intermediate reaction products):

$$XeF_2(g) \rightleftarrows XeF_2(p), \tag{7}$$

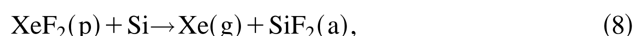

$$XeF_2(p) + Si \rightarrow Xe(g) + SiF_2(a), \tag{8}$$

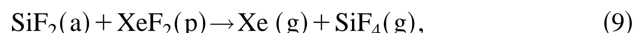

$$SiF_2(a) + XeF_2(p) \rightarrow Xe\,(g) + SiF_4(g), \tag{9}$$

$$SiF_2(a) \rightarrow SiF_2(g). \tag{10}$$

First, the incident $XeF_2(g)$ is trapped in a precursor state, $XeF_2(p)$, from which it can either desorb back into the gas phase or react [Eq. (7)]. This reaction can be dissociation on

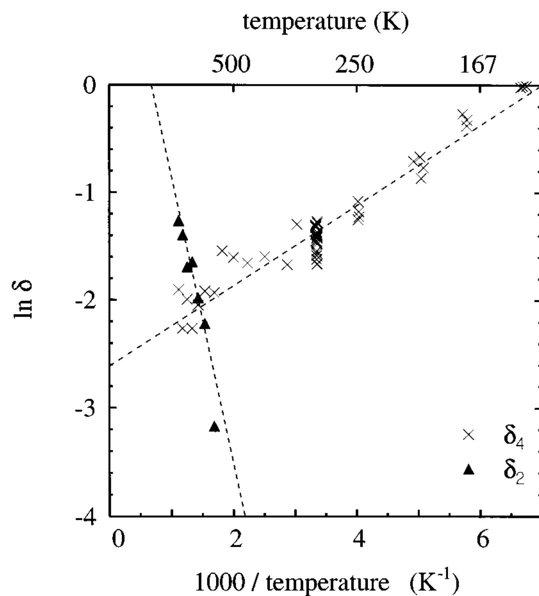

FIG. 11. Arrhenius plot of the production coefficients δ_4 and δ_2. The dashed lines represent a least squares fit.

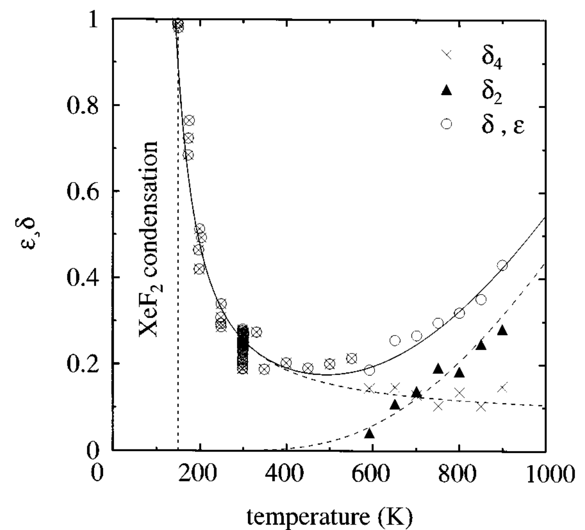

FIG. 12. Temperature dependence of ϵ, δ_4, and δ_2, assuming that desorption of XeF$_2$ and SiF$_2$ are the rate limiting steps.

bare silicon sites resulting in silicon fluorides [Eq. (8)] or reaction with already fluorinated sites to create the etch product SiF_4 [Eq. (9)]. At the same time, when the temperature is high enough, incomplete silicon fluoride species can desorb spontaneously [Eq. (10)]. Of course, these reaction steps must be considered to be not more than a rough description of the overall behavior. In reality the SiF_x reaction layer does not consist of SiF_2 species, but of a complex chain structure of SiF-, SiF_2- and SiF_3-species, created in a sequential fluorination mechanism.[5] Therefore the production mechanisms of SiF_4 and SiF_2 will also be much more complex. Furthermore, we leave aside the possibility of XeF_2-condensation.

In this 4-step model we can distinguish two limiting cases. At low temperatures there is no desorption of SiF_2, the fluorine content of the reaction layer is constant and the etch rate, i.e., SiF_4 production, is limited by the XeF_2-precursor concentration.[27,28] At high temperatures the change in the desorption rate of the XeF_2-precursor can be neglected and the etch rate is limited by the desorption of SiF_2. This results in the following equations:

$$\delta_4 = \delta_{4,0} e^{E_d / k_B T}, \tag{11}$$

$$\delta_2 = \delta_{2,0} e^{-E_2 / k_B T}, \tag{12}$$

with E_d and E_2 the activation energies of desorption for the XeF_2-precursor and the SiF_2-species, respectively. Figure 11 is an Arrhenius plot of the experimental data; we observe that these equations describe the temperature dependence quite well. The optimal values of E_d and E_2, corresponding to the dashed curves, are

$$E_d = 32 \pm 4 \text{ meV}, \tag{13}$$

$$E_2 = 260 \pm 30 \text{ meV}. \tag{14}$$

The value for E_d is 5.5% of the XeF_2 vaporization energy [Eq. (2)], which seems reasonable. The SiF_2 desorption energy is in reasonable agreement with the value observed by Dagata *et al.*[11] (290±20 meV).

In Fig. 12 the reaction coefficient ϵ (or the total production coefficient δ) is compared to the sum of Eq. (11) and Eq. (12). We find that the temperature dependence of the Si/XeF_2-reaction is described surprisingly well by the sum of the high and low temperature approximation. The discrepancy of the 500 K and 550 K data points for δ_4 is possibly caused by a slight SiF_2 contribution at these temperatures. As described in section V, the calibration method is based on the assumption that there is no significant SiF_2 contribution below 600 K. Another possible explanation is the breakdown of the SiF_x reaction layer at these temperatures.

B. Reaction layer

We will discuss the formation of the reaction layer within the framework of the chain model, which was presented in a previous paper[8] to describe the reaction layer formation at room temperature. In this model the reaction layer formation consists of two steps. First a monolayer of SiF_p-species is formed; this is a fast process. Then there is a slow transition from the monolayer to a multilayer of Si_xF_q-chains. The parameters p and q represent the average number of fluorine atoms per surface silicon site. These processes can be expressed by the following rate equations:

$$\frac{\partial[SiF_p]}{\partial t} = k_f \Phi(XeF_2)\left(1 - \frac{[SiF_p]}{\rho N_0} - \frac{[Si_xF_q]}{\rho N_0}\right) - k_c \Phi(XeF_2)\frac{[SiF_p]}{\rho N_0}, \tag{15}$$

$$\frac{\partial[Si_xF_q]}{\partial t} = k_c \Phi(XeF_2)\frac{[SiF_p]}{\rho N_0}, \tag{16}$$

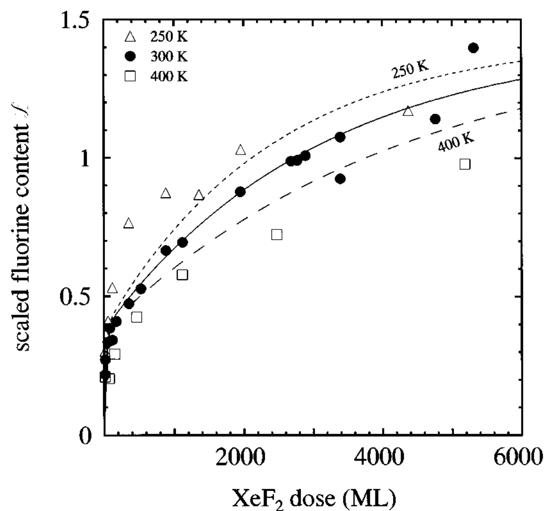

FIG. 13. Comparison between the reaction layer formation for sample temperatures of 250 K and 400 K, predicted by the chain model extended with the XeF$_2$-precursor (dashed curves), and the experimental data. The 300 K data and the chain-model fit (solid curve) are shown for comparison.

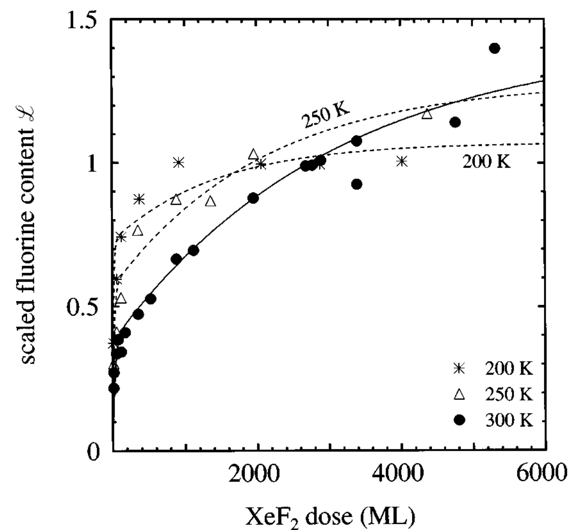

FIG. 14. Fit of the scaled fluorine content $\mathscr{L}$ of the reaction layer as a function of XeF$_2$-dose for sample temperatures of 300 K and below. The solid (300 K) and dashed curves (as labeled in the figure) represent the fit with the precursor chain model, using p and q as free parameters.

in which $[SiF_p]$ is the surface concentration of SiF_p-species and $[Si_xF_q]$ of Si_xF_q-chains. These concentrations are normalized to the surface concentration of silicon atoms ρN_0. The quantity N_0 is the Si surface concentration on a smooth surface ($N_0=1$ ML) and ρ indicates the roughness of the surface ($\rho \geqslant 1$). The parameters k_f and k_c are the rate constants for surface fluorination and chain formation, respectively. The fit that was obtained with this model for the 300 K data[8] is shown in Figs. 5 and 6.

When we compare the data at temperatures below and above room temperature to the 300 K fit with the chain model, we observe that the initial increase in the fluorine content is faster for lower temperatures and slower for higher temperatures (Figs. 5 and 6). This again indicates the presence of a XeF$_2$-precursor. An increase in the XeF$_2$-precursor concentration for decreasing temperature will cause the reaction layer formation to occur at a lower XeF$_2$-dose, and thus show a faster increase. The simplest way to implement this XeF$_2$-precursor in the chain model is to replace the XeF$_2$-flux $\Phi(XeF_2)$ by the steady-state XeF$_2$-precursor concentration $[XeF_2]$, which can be approximated by

$$[XeF_2]=[XeF_2]_0 e^{E_d/k_B T}. \quad (17)$$

When we use the activation energy E_d from Eq. (13), the predicted dose dependence for sample temperatures of 250 K and 400 K is given by the dashed curves in Fig. 13.

Clearly the precursor effect is not sufficient to explain the temperature dependence of the reaction layer formation. This is not surprising since both the etch rate and the product distribution change significantly as a function of temperature. This means that probably the parameters p and q should also be temperature dependent. When we use these two parameters to fit the reaction layer formation with the precursor chain model, we obtain the dashed curves in Figs. 14 and 15. In this way reasonable fits are obtained over the whole temperature range. The 175 K data are left aside since they have a totally different character due to the condensation of XeF$_2$.

In Fig. 16 the values of p and q that correspond to the fits in Figs. 14 and 15 are plotted as a function of sample temperature. These numbers can be interpreted as the F-atom coverage in ML of a smooth surface after the initial adsorption phase (p) and in the steady state multilayer regime (q). The parameter p decreases monotonically from a fully saturated SiF$_3$ coverage at 200 K ($p=3$) to a submonolayer coverage at 700 K ($p<1$). The parameter q, representing the steady-state layer, shows a maximum at room temperature. This effect is not so clear in the 2400 ML data of Fig. 4.

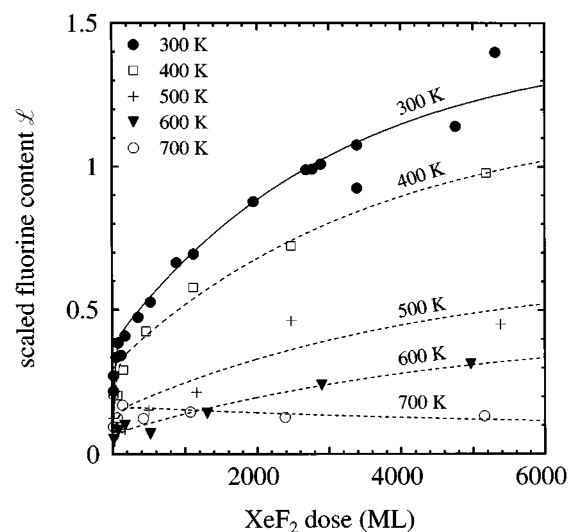

FIG. 15. Scaled fluorine content $\mathscr{L}$ of the reaction layer as a function of XeF$_2$-dose for sample temperatures of 300 K and above. Again the solid (300 K) and dashed curves (as labeled in the figure) represent the fit with the precursor chain model, using p and q as free parameters.

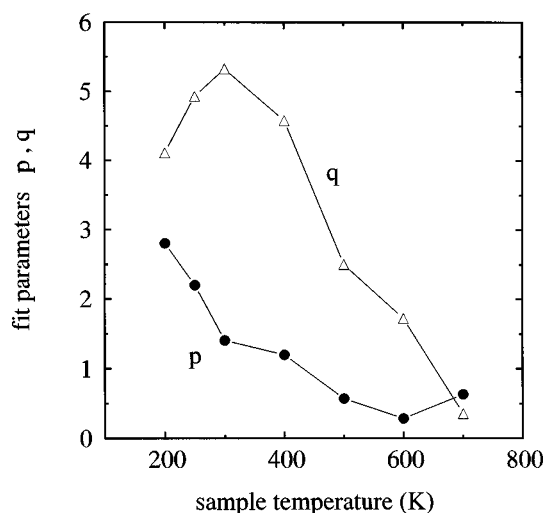

FIG. 16. Dependence of the parameters p (corresponding to SiF_p) and q (corresponding to Si_xF_q) in the precursor chain model on sample temperature.

From the dose dependences in Fig. 14 we conclude that 2400 ML of exposure is just an unfortunate choice. The decrease of q for low temperatures may be explained by the strong increase in etch rate in this regime, leaving insufficient time for chain formation to occur. It is also possible that the penetration of fluorine into the silicon lattice becomes more difficult at low temperatures. For the decrease at high temperatures the desorption of loosely bound species could be responsible. Another possible explanation is the healing of defects within the layer. The maximum in q coincides with the maximum in the Si_2F_6-contribution as was observed in the SiF_3^+/SiF^+ signal ratio and in the F-atom experiments by Winters and Coburn.[1] This seems plausible, since a multilayer is necessary to form Si_2F_6.

VII. CONCLUSIONS

We have presented a detailed study on all aspects of the temperature dependence of the Si/XeF$_2$ reaction. It was found that the steady-state reaction layer has a maximum fluorine content at room temperature. This content corresponds to 5.5 ML for a smooth surface, indicating a Si_xF_y multilayer structure. For increasing temperatures it decreases to a submonolayer coverage above 700 K. For decreasing temperatures there is also a small decrease, but below 200 K the fluorine content increases again due to XeF_2 condensation. The formation of this reaction layer is faster for decreasing temperatures, indicating a precursor mediated mechanism. A reaction mechanism involving a XeF_2-precursor is also necessary to explain the strong increase in reaction probability with decreasing temperature, from 20% at 300 K up to 100% at 150 K. In a simple model the activation energy for desorption of the precursor was estimated to be 32 ± 4 meV. For temperatures above 600 K the reaction probability increases again up to 45% at 900 K. This can be explained by the production of SiF_2 with an activation energy of 260 ± 30 meV.

For temperatures of 150 K and below, the etching process is initially very efficient: all of the XeF_2 is used to produce SiF_4. However, after a certain time of exposure the small fraction of XeF_2 that condenses on the surface is accumulated to form a XeF_2 overlayer that blocks the reaction. It may be possible to achieve a continuous efficient etch process at these temperatures by simultaneously radiating the surface with photons or ions. For instance it was shown very recently by Li *et al.*[29] that the room temperature Si/XeF_2-reaction can be enhanced significantly using VUV-light in the spectral range of 105–122 nm. Possibly this can even have a technological application as a low-damage direct-writing technique. Irradiated areas will have a high etch rate, while the etch reaction is completely blocked by XeF_2 condensation at non-irradiated areas.

ACKNOWLEDGMENT

The authors wish to thank H. H. Brongersma (Physics of Surfaces and Interfaces, Eindhoven University of Technology) for many helpful discussions.

[1]H. F. Winters and J. W. Coburn, Surf. Sci. Rep. **14**, 161 (1992).
[2]T. J. Chuang, H. F. Winters, and J. W. Coburn, Appl. Surf. Sci. **2**, 514 (1978).
[3]F. R. McFeely, J. F. Morar, N. D. Shinn, G. Landgren, and F. J. Himpsel, Phys. Rev. B **30**, 764 (1984).
[4]F. R. McFeely, J. F. Morar, and F. J. Himpsel, Surf. Sci. **165**, 277 (1986).
[5]C. W. Lo, D. K. Shuh, V. Chakarian, T. D. Durbin, P. R. Varekamp, and J. A. Yarmoff, Phys. Rev. B **47**, 15 648 (1993).
[6]J. R. Engstrom, M. M. Nelson, and T. Engel, Surf. Sci. **215**, 437 (1989).
[7]M. J. M. Vugts, G. J. P. Joosten, A. van Oosterum, H. A. J. Senhorst, and H. C. W. Beijerinck, J. Vac. Sci. Technol. A **12**, 2999 (1994).
[8]M. J. M. Vugts, M. F. A. Eurlings, L. J. F. Hermans, and H. C. W. Beijerinck, J. Vac. Sci. Technol. A **14**, 2780 (1996).
[9]F. A. Houle, J. Appl. Phys. **60**, 3018 (1986).
[10]H. F. Winters and I. C. Plumb, J. Vac. Sci. Technol. B **9**, 197 (1991).
[11]J. A. Dagata, D. W. Squire, C. S. Dulcey, D. S. Y. Hsu, and M. C. Lin, J. Vac. Sci. Technol. B **5**, 1495 (1987).
[12]D. E. Ibbotson, D. L. Flamm, J. A. Mucha, and V. M. Donnely, Appl. Phys. Lett. **44**, 1129 (1984).
[13]V. M. Bermudez, J. Vac. Sci. Technol. A **10**, 3478 (1992).
[14]T. J. Chuang, J. Appl. Phys. **51**, 2614 (1980).
[15]S. Tachi, K. Tsujimoto, and S. Okudaira, Appl. Phys. Lett. **52**, 616 (1988); **53**, 1665 (1988).
[16]T. Mizutani, T. Yunogami, and K. Tsujimoto, Appl. Phys. Lett. **57**, 1654 (1990).
[17]R. A. B. Devine, Appl. Phys. Lett. **57**, 2564 (1990).
[18]T. D. Bestwick, G. S. Oehrlein, and D. Angell, Appl. Phys. Lett. **57**, 431 (1990).
[19]S. Tachi, K. Tsujimoto, S. Arai, and T. Kure, J. Vac. Sci. Technol. A **9**, 796 (1991).
[20]C. B. Mullins and J. W. Coburn, J. Appl. Phys. **76**, 7562 (1994).
[21]P. A. Redhead, Vacuum **12**, 203 (1962).
[22]F. Schreiner, G. N. McDonald, and C. L. Chernick, J. Phys. Chem. **72**, 1162 (1968).
[23]R. B. Jackman, R. J. Price, and J. S. Foord, Appl. Surf. Sci. **36**, 296 (1989).
[24]P. L. Timms, R. A. Kent, T. C. Ehlert, and J. L. Margrave, J. Am. Chem. Soc. **87**, 2824 (1965).
[25]H. F. Winters and D. Haarer, Phys. Rev. B **36** 6613 (1987); **37**, 10 379 (1988).
[26]J. A. Yarmoff and F. R. McFeely, Phys. Rev. B **38**, 2057 (1988).
[27]H. F. Winters and J. W. Coburn, Appl. Phys. Lett. **34**, 70 (1979).
[28]K. Ninomiya, K. Suzuki, S. Nishimatsu, and O. Okada, J. Appl. Phys. **58**, 1177 (1985).
[29]B. Li, U. Streller, H.-P. Krause, I. Twesten, and N. Schwentner, J. Appl. Phys. **77**, 350 (1995).